PHILOSOPHICAL MAGAZINE A, 1998, VOL. 77, NO. 1, 55–65

Atomistic study of the (001), 90° twist boundary in silicon

By A. YU. BELOV†, D. CONRAD, K. SCHEERSCHMIDT and U. GÖSELE

Max Planck Institute of Microstructure Physics, Weinberg 2, D-06120 Halle, Germany

[*Received 5 December 1996 and accepted in revised form 21 April 1997*]

ABSTRACT

A new type of a structural unit (the $\bar{4}2m$ dreidl) is proposed on the basis of molecular dynamics simulations for the core model of the (001), 90° twist grain boundary in silicon. The structural unit resembles a polyhedron in which some edges, not corresponding to bonds between atoms, are absent. The dreidl has the $\bar{4}2m$ (D_{2d}) point-group symmetry and consists of 14 atoms which form eight five-membered rings maintaining tetrahedral bonding in the boundary core. Molecular dynamics simulations with the empirical Tersoff potential were performed to evaluate the energy of the (001), 90° twist boundary at $T = 0$ K. The effect of both rigid-body translations parallel to the grain boundary plane and alternative reconstructions involving conventional structural units was investigated. Despite the high degree of dimerization the twist boundary was found to have a low energy compared with structural models of twist grain boundaries in silicon previously studied.

§ 1. INTRODUCTION

In general, complex symmetry properties of a crystal structure provide a variety of ways to disturb the crystalline order in the structure with a minimal change in its energy by creating various lattice defects. The more elements the space symmetry group contains, the more types of defects may be produced in the structure, with a symmetry element lost generating a particular type of lattice defect. In particular, a specific type of a planar defect can occur in non-symmorphic crystals of diamond cubic lattice (space symmetry group, $Fd\bar{3}m$) such as Si, Ge or C owing to the presence of a fourfold screw axis 4_1. Owing to this symmetry element, when a single-atomic layer normal to the screw axis (i.e. a (004) plane) is removed in a diamond-lattice crystal, the two half-crystals adjacent to the layer turn out to be rotated by 90° about it. The subsequent joining of the two half-crystals by a translation towards each other results in the (001), 90° twist grain boundary. It can arise from a 90° rotation of one part of a crystal or from the aggregation of point defects (vacancies or interstitial atoms), that is without real rotation. Another important feature of this twist boundary stems from the fact that the 90° rotation changes the normal sequence of (004) layers in the diamond lattice, thus creating a stacking fault in the (001) plane. Indeed, the atomic arrangement in the diamond lattice can be envisaged as a helix with the stacking sequence abcdabcd... of four basic layers a, b, c and d along its axis which coincides with the fourfold screw. The basic layers occupy in the cubic unit cell the positions $z = 0, \frac{1}{4}, \frac{1}{2}$ and $\frac{3}{4}$ respectively, and each layer

† On leave from Institute of Crystallography, Russian Academy of Sciences, Moscow, Russia.

in the sequence abcd... can be obtained by 90° counter-clockwise rotation of the preceding layer about the helix axis and a subsequent translation along it by a quarter of the lattice parameter. Therefore, the counter-clockwise rotation of the upper half-crystal by 90° about 4_1 changes the lettering of each layer above the rotation plane according to the rule $a \to b \to c \to d \to a$. On the assumption that the letters of the part below the rotation plane remain the same, this procedure can be represented as follows:

$$\begin{array}{cccccccc} a & b & c & d & a & b & c & d \\ & & & & \downarrow & \downarrow & \downarrow & \downarrow \\ & & & & b & c & d & a \end{array} \qquad (1)$$

resulting in a stacking sequence

$$a\ b\ c\ d|\ \ |b\ c\ d\ a\ \cdots \qquad (2)$$

with a removed a layer (unstable intrinsic stacking fault). In turn, 90° clockwise rotation of the upper half-crystal changes the lettering above the rotation plane as

$$\begin{array}{cccccccc} a & b & c & d & a & b & c & d \\ & & & & \downarrow & \downarrow & \downarrow & \downarrow \\ & & & & d & a & b & c \end{array} \qquad (3)$$

such that a stacking sequence

$$a\ b\ c\ d\ |d|\ a\ b\ c\ \cdots \qquad (4)$$

with an inserted d layer (extrinsic stacking fault) occurs.

Here we report an atomic structure of the (001), 90° twist boundary in Si predicted by classical molecular dynamics (MD) simulations with the empirical many-body potential of Tersoff (1989). The present study is motivated by a considerable interest in the atomic and electronic structures of synthetically made (001) interfaces in Si, since a Si(001) wafer is the most common material used in wafer-bonding technology (Gösele *et al.* 1995). As is known, a vicinal Si(001) surface consists of terrace-like domains of dimer rows and atomic steps (along [110] or/and [$\bar{1}$10]) separating the domains and accommodating the miscut angle. According to Chadi (1987), there are two types of stable step: single-layer steps S_A and S_B, which rotate the dimerization direction in the neighbouring domains, and double-layer steps D_A and D_B, which conserve it. The former are known to become energetically favourable at miscut angles smaller than 1°. Thus, the (001), 90° twist boundary may occur if a flat (001) surface adheres to a surface with a single-layer step S_A to restore perfect bonding across one terrace. According to figure 1, this procedure gives rise to a stacking fault of either intrinsic (vacancy) or extrinsic (interstitial) type, depending on the mutual orientation of dimer rows on the adjacent surfaces of upper and lower crystals. The intrinsic stacking fault occurs if dimerization directions of the upper crystal surface and the upper terrace of the lower crystal coincide (figure 1 (*a*)). Otherwise, the extrinsic stacking fault occurs, as shown in figure 1 (*b*).

Furthermore, the study of the {001} extrinsic stacking fault was encouraged by a considerable interest in the atomic structure and energy of agglomerations of self-interstitials in Si and Ge, which occur as planar and/or rod-like defects after light-ion implantation or electron irradiation. Although interstitial atoms mostly aggregate on the {113} habit plane (Burret 1987, Takeda 1991, Takeda *et al.* 1994, Aseev *et al.*

Fig. 1

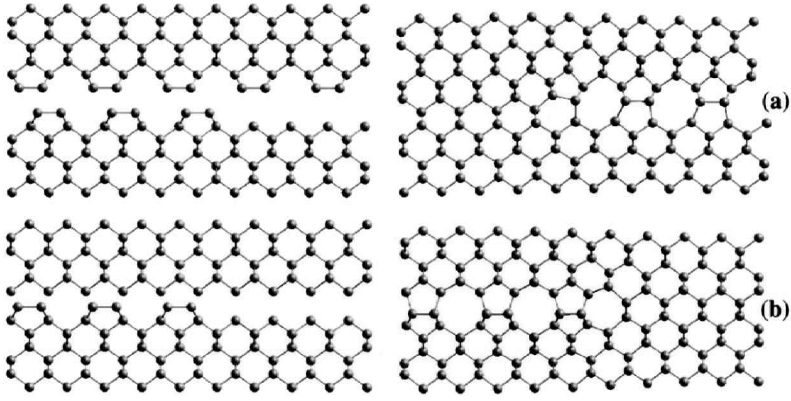

A single-layer step S_A adheres to a flat (001) surface to form an intrinsic (*a*) or an extrinsic (*b*) stacking fault.

1994), interstitial agglomerations with the {001} habit plane have been reported too (Pasemann *et al.* 1983, Muto and Takeda 1995). Hence, although direct high-resolution electron microscopy (HREM) observations are very rare for twist grain boundaries in Si and Ge (Sutton 1991), there is some experimental information as to the structure of interstitial planar defects. Recently energy minimization calculations for the {113} interstitial defect in Si have been carried out using empirical potentials (Kohyama and Takeda 1992, Parisini and Burret 1993) and the tight-binding method (Kohyama and Takeda 1995). Therefore, from energy calculations of the {001} extrinsic stacking fault and a respective comparison with the above results for the {113} one could elucidate the observed hierarchy of the habit planes in the aggregation of self-interstitial atoms.

§ 2. Simulation procedures

The energy minimization simulation of the atomic structure in the (001), 90° twist boundary core at $T = 0\,\mathrm{K}$ was performed using constant-energy-volume MD, with the velocities being rescaled to remove the kinetic energy. The fifth-order predictor–corrector algorithm of Gear was employed in the integration scheme with time step of $2{\cdot}5 \times 10^{-16}$ or $1{\cdot}0 \times 10^{-15}$ s. The empirical interatomic potential of Tersoff (1989) was chosen which was motivated by comparative studies of two reconstructions of the 90° partial dislocation core in Si. In agreement with *ab-initio* pseudopotential calculations (Bigger *et al.* 1992), the potential of Tersoff predicts the asymmetric reconstruction with fourfold-coordinated atoms, whereas the Stillinger–Weber (1985) potential, in contrast, supports the symmetric quasifivefold-coordinated reconstruction (Duesbery *et al.* 1991). However, the Stillinger–Weber potential with the larger cut-off radius than the Tersoff potential was also employed in the present study.

The computational cell $L_x \times L_y \times L_z$ contains a block of 69 single-atomic (004) layers (4968 atoms) and has dimensions $L_x = 12a_0$ and $L_y = 6a_0$ ($a_0 = 3{\cdot}84$ Å is the shortest translation in Si) in the directions $x = [110]$ and $y = [\bar{1}10]$ respectively. Periodic boundary conditions are imposed in the directions x and y, whereas the

dimension L_z in the direction $z = [001]$ was chosen so as to keep the upper and lower surfaces of the block free. This kind of border condition allows for relaxation along z and enables the free volume associated with the grain boundary to be evaluated. The initial atomic configuration (model A) was constructed as follows.

(1) An a layer at the centre of the 70-layer block is removed, which divides the original block into two half-crystals.
(2) The adjacent surfaces of two half-crystals are reconstructed to form rows of dimers, which corresponds to wafer-bonding modelling.
(3) The upper crystal is translated by $a/2 = 2{\cdot}715$ Å along $[100]$, where $a = 5{\cdot}43$ Å is the lattice parameter of Si, and by $a/4 = 1{\cdot}358$ Å along $[00\bar{1}]$ (towards the lower half-crystal). Apart from the atomic displacements due to formation of the dimer bonds, initial positions of atoms in model A are given by eqn. (4), since the translation of the upper half-crystal by the vector $(a/2)[100]$ changes the stacking sequence (2) according to the rule

$$\begin{array}{cccccccc} a & b & c & d & b & c & d & a \\ & & & & \downarrow & \downarrow & \downarrow & \downarrow \\ & & & & d & a & b & c \end{array} \qquad (5)$$

and thereby transforms it into the extrinsic stacking fault (4).

The effect of rigid-body translations parallel to the boundary plane on the energy of the twist boundary was investigated by a preliminary translation of the upper half-crystal in model A by vector $(a_0/2)[110]$. This procedure changes the lettering order as

$$\begin{array}{cccccccc} a & b & c & d & d & a & b & c \\ & & & & \downarrow & \downarrow & \downarrow & \downarrow \\ & & & & c & b & a & d \end{array} \qquad (6)$$

and gives rise to a twin $abc|d|cbad\ldots$. The optimum translation is automatically determined during relaxation. Since there is a symmetry axis $\bar{4}$ in model A, translation in the perpendicular direction does not result in a new atomic configuration. The configuration obtained allows two types of reconstruction: with quasifivefold-coordinated atoms (model B) and with only fourfold-coordinated atoms (model C). Structural model B, found in MD simulations with a modified Stillinger–Weber potential (Conrad *et al.* 1996), occurs if the dimer bonds on one of the adjacent surfaces are broken, whereas structural model C results from the procedure proposed by Tan (1981) for the intermediate defect configurations, resembling his model of the {113} stacking fault. The initial positions of atoms in the structural models B and C were prepared by MD simulations using the code Cerius3.2, which employs the Keating valence force field and enables the prescribed topology of the bond network to be conserved in the course of MD run. In simulations with the Tersoff and Stillinger–Weber potentials, bonds are only conceptual.

§ 3. Discussion of results

As previous simulations showed (Phillpot and Wolf 1989, Tarnow *et al.* 1990, Cheikh *et al.* 1991, Ralantoson *et al.* 1993, Kohyama *et al.* 1993, Kohyama and Yamamoto 1994, Kohyama 1996), in Si and Ge the twist boundaries generally

Table 1. Energy and structural disorder for different models of the (001), 90° twist boundary and coincident site lattice twist boundaries (Kohyama 1996) (tight-binding method).

Boundary	Rotation angle (degrees)	E_{gb} ($J\,m^{-2}$)	Bond stretching (%)	Bond bending (degrees)
⟨001⟩, model A	90·0	0·85	- 1·4 to + 3·8	- 12·4 to + 15·9
⟨001⟩, model B	90·0	1·02	Coordination defects	
⟨001⟩, model C_2	90·0	1·94	- 6·9 to + 10·1	- 59·0 to + 35·1
⟨001⟩, model C_6	90·0	1·98	- 2·1 to + 6·0	- 33·2 to + 19·1
⟨001⟩, model D_2	90·0	1·53	Coordination defects	
⟨001⟩, model D_6	90·0	1·20	Coordination defects	
⟨111⟩, $\Sigma = 7$	38·2	1·28	- 1·4 to + 4·6	- 23·5 to + 21·3
⟨111⟩, $\Sigma = 7$	98·2	1·28	- 1·4 to + 4·9	- 25·0 to + 22·1
⟨011⟩, $\Sigma = 3$	109·5	1·02	- 2·4 to + 2·0	- 35·5 to + 28·5
⟨001⟩, $\Sigma = 5$	36·9	2·05	- 2·5 to + 16·0	- 24·4 to + 37·3
⟨001⟩, $\Sigma = 5$	53·1	2·34	- 1·5 to + 14·8	- 24·7 to + 49·8

exhibit a higher structural disorder (distorted bonds and coordination defects) than tilt boundaries do. Thus stable structural units with only fourfold-coordinated atoms, similar to those for tilt boundaries, are difficult to construct. Even when such structural units are possible, high bond distortions give rise to interfacial energies large relatively to those typical of tilt boundaries. However, a low-energy structural unit turns out to be possible for the (001), 90° twist boundary. The results of the energy minimization simulations for the structural models A, B, C and D at $T = 0$ K are summarized in table 1, where the energies and characteristics of structural disorder for some other structural models of twist boundaries (without coordination defects) are reproduced for comparison from the review by Kohyama (1996). The energy minimum is achieved in model A (fig. 2(*a*)) which retains all dimer bonds between atoms in the same grain. Also, new bonds are formed across the grain boundary to recover the fourfold coordination for all atoms in the grain-boundary core. A similar tendency to lower the energy by forming dimer bonds parallel to the boundary rather than bonds across the boundary has been found in *ab initio* pseudopotential calculations by Tarnow *et al.* (1990) for $\Sigma = 5$, (001) twist boundaries (36·9° and 53·1°) in Ge. The grain-boundary region in model A is (2 × 2) reconstructed and can be imagined as consisting of arrays of structural units shown in fig. 3. This structural unit is called dreidl, following the paper by Mostoller *et al.* (1994), where a similar closed structure, the *mm*2 dreidl, composed of five- and seven-membered atomic rings (18 atoms) and having the point symmetry group *mm*2 (C_{2v}) was shown to occur at the intersection of two orthogonal edge dislocations. The dreidl of fig. 3 consists of 14 atoms, which form eight five-membered rings. It has the improper fourfold symmetry axis 4 and belongs to the point group 42*m* (D_{2d}). According to table 1, the dreidl fits two rotated half-crystals with a minimal structural disorder, only dimer bonds of the length $d = 2{\cdot}44$ Å are moderately stretched. Therefore it is a suitable 'twist unit' for the 90° rotation in the diamond lattice.

Model B (fig. 2(*b*)) was found to have an energy only about 19% higher energy than that of model A despite the presence of coordination defects and larger bond distortions. The grain-boundary region is (2 × 1) reconstructed, containing quasi-fivefold-coordinated atoms with four neighbours at a distance of 2·50 Å, and one neighbour (floating bond) at a somewhat larger distance $d = 2{\cdot}55$ Å, which is the

Fig. 2

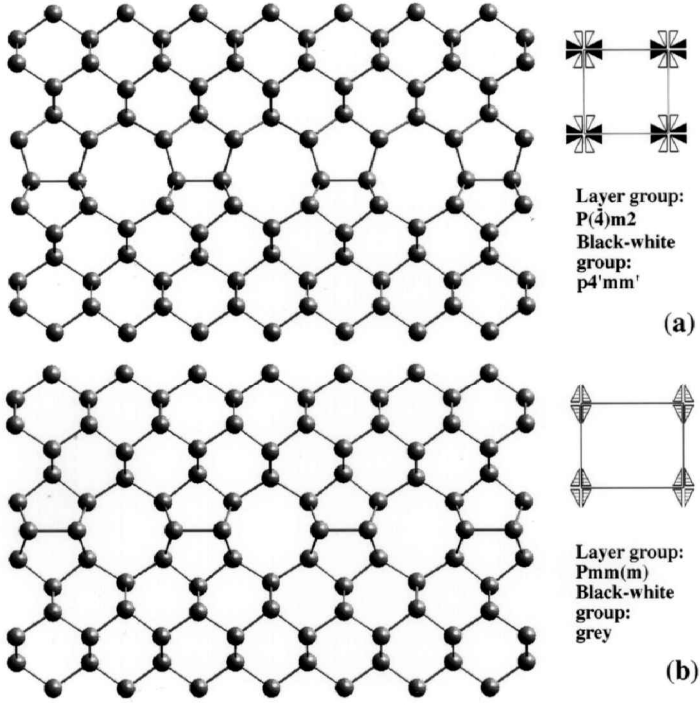

Structural models (*a*) A and (*b*) B of the (001), 90° twist boundary. Layer group symbols and planar black–white group symbols of the grain boundary core are given according to Grell *et al.* (1988).

Fig. 3

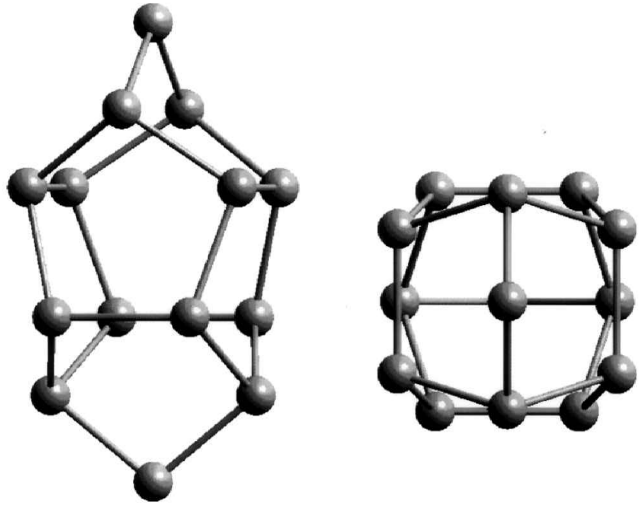

Dreidl: closed structure with the point group $\bar{4}2m$, black–white point group $\bar{4}'2'm$ (white and black atoms belong to the upper and lower half-crystals respectively).

length of the unbroken dimer bond. The energy minimization for models A and B was also performed using the potential of Stillinger and Weber, which is known (Phillpot and Wolf 1989, Kohyama and Yamamoto 1994) to favour overcoordinated structures, especially those containing fivefold-coordinated defects typical of amorphous Si, since this potential is parametrized to reproduce the structure of liquid. However, in the present calculations the Stillinger–Weber potential gives rise to energies for model A (E_{gb} = 0·806 J m^{-2}) and model B (E_{gb} = 1·044 J m^{-2}) similar to those obtained with the potential of Tersoff. Hence the tendency for the Stillinger–Weber potential to produce overcoordinated structures is not confirmed in this case.

Relaxation of model C created by using the Keating valence force field reveals complicated metastable configurations with large energies and bond distortions, but without coordination defects. Two metastable configurations were obtained with the Tersoff potential: C_2 with the reconstruction (2 × 1), and C_6 with the reconstruction (6 × 1). The two configurations (illustrated in figs. 4(*a*) and (*b*) respectively) have similar *y* projections but differ in atomic displacements along the *y* axis. Models C_2 and C_6 contain the conventional structural units such as alternating pairs of five- and seven-membered rings separated by six-membered rings. Such a structure resembles an array of parallel dipoles of edge dislocations. The energies of these two models exceed the energy of model A more than twice, correlating with the value 1·83 J m^{-2} obtained by Phillpot and Wolf (1989) with the Stillinger–Weber potential for an unreconstructed (001), 90° twist boundary. As follows from table 1, model C_2 has a somewhat lower energy than model C_6 in spite of larger bond distortions. This might be explained by the fact that some atoms in the boundary core of model C_2 are actually fivefold rather than fourfold coordinated, and in this case the Tersoff potential favours the overcoordinated structure. However, it is more important that models C_2 and C_6 turn out to be unstable for the Stillinger–Weber potential. The

Fig. 4

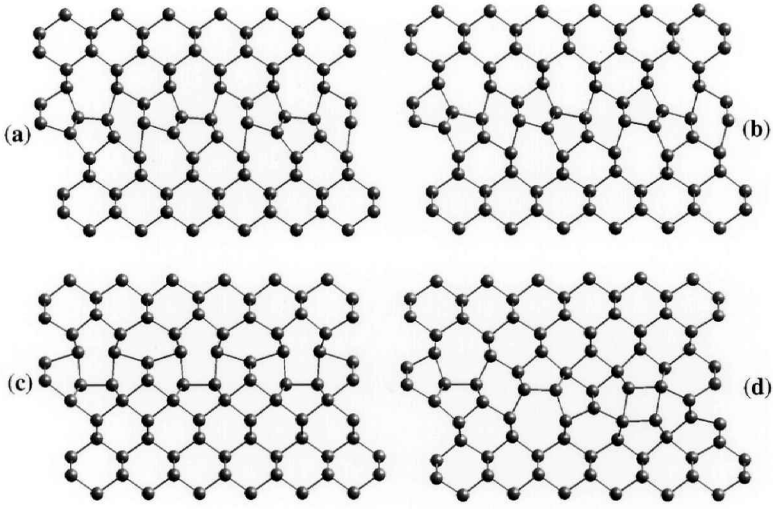

Structural models (*a*) C_2, (*b*) C_6, (*c*) D_2 and (*d*) D_6 of the (001), 90° twist boundary.

corresponding energy minima, configurations D_2 and D_6, were achieved in the course of two successive MD runs with the Stillinger–Weber and Tersoff potentials. According to table 1, these models have significantly lower energies than C_2 and C_6, although there are coordination defects in the grain-boundary core (figs. 4(*c*) and (*d*)). One should also note that the reconstruction (6×1) correlates with size $L_x = 12a_0$ of the computational cell, which is a multiple of six. This probably means that the tendency to lower the grain-boundary energy by forming an aperiodic structure is suppressed by the periodic boundary conditions.

§ 4. Concluding remarks

It is well recognized that in covalently bonded materials the atomic structures of grain boundaries are related to their electronic structures and that the stability of grain boundaries depends upon the formation of stable structural units (for example Sutton and Balluffi (1995) and references therein) consisting of atomic rings without dangling bonds, and with only small bond distortions. This idea, in its simplest form of the 'stick-and-ball' model, was first used by Hornstra (1959, 1960) to predict the basic structural models of dislocations and tilt boundaries. The present study allows some conclusions as to the stability of different structural units to be drawn from the properties of models A and C constructed according to this principle, and to elucidate the role of eight-membered rings in stabilizing the structures. Model A composed of five- and eight-membered rings in [110] projection is the most stable configuration, since the introduction of the eight-membered rings allows one to optimize the angular bond distortions and thereby to reduce the grain-boundary energy. Model C consisting of only five-, six- and seven-membered rings is a high-energy metastable state for the Tersoff potential, and not at all stable for the Stillinger–Weber potential. Similar trends have been pointed out (Kohyama and Takeda 1992) for the {113} interstitial planar defect. The model of Tan (1981) made up of five- and seven-membered rings has a considerably higher energy (Aseev *et al.* 1994) than that of Takeda (1991), who introduced eight-membered rings to stabilize the structure.

The results of our simulations listed in table 2 allow one to elucidate the influence of the grain-boundary reconstruction on the free volume, which is the volume difference of the crystal with the twist boundary, and the corresponding perfect crystal. By now, many attempts have been made to relate the free volume to structural features and the energy of twist boundaries. In particular, positive volume expansions have been reported for different models of (001) twist boundaries, both unreconstructed (Phillpot and Wolf 1989) and reconstructed (Kohyama and

Table 2. Free volume for different reconstructions of the (001), 90° twist boundary.

Model	Reconstruction	Volume expansion (Å per unit area)
A	(2×2)	0·64
B	(2×1)	0·55
C_2	(2×1)	- 0·33
C_6	(6×1)	- 0·33
D_2	(2×1)	- 0·33
D_6	(6×1)	- 0·27

Yamamoto 1994), whereas some other twist boundaries, (111) and (511), were shown to undergo a contraction (Phillpot and Wolf 1989, Cheikh *et al.* 1991, Kohyama and Yamamoto 1994). According to table 2, the (001), 90° twist boundary can undergo both expansion and contraction depending on the type of reconstruction. The dominating factor is the directionality of bonds. The grain boundary tends to optimize angular bond distortions close to the nearest energy minimum, which is possible by either expansion or contraction.

Finally, we discuss the energetics of aggregation of self-interstitial atoms in Si. The tight-binding calculations of Kohyama and Takeda (1995) for Si yield the value $E_{gb} = 0{\cdot}60\,J\,m^{-2}$ for two structural models of the {113} interstitial planar defect,

Fig. 5

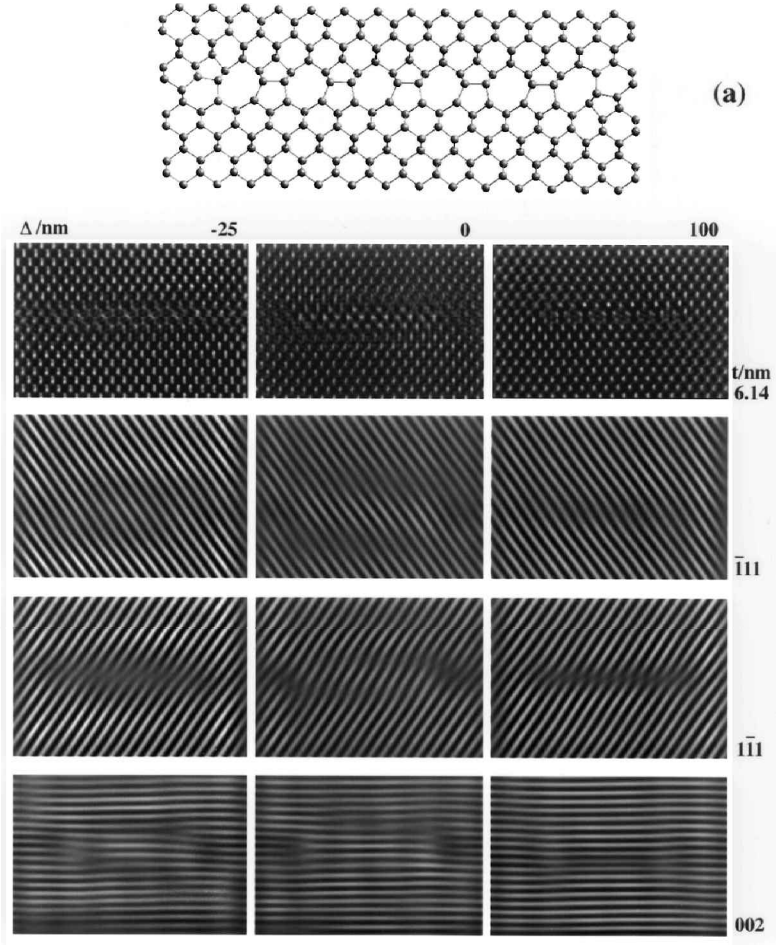

Simulated $[\bar{1}10]$ HREM and filtered images of the (*a*) intrinsic and (*b*) extrinsic stacking faults. Structural models (*a*) and (*b*) are relaxed using the Tersoff potential. There are no dangling bonds in cores of the partial dislocations situated at the edges of the stacking faults. Imaging conditions are specified by the electron beam energy $E = 200\,kV$, spherical aberration $C_s = 1{\cdot}2\,mm$, the defocus value Δ (nm) and the specimen thickness t (nm).

(*Continued overleaf*)

namely $|IO|_2$ and $|IIO|_2$ which involve eight-membered rings. Similar values $0{\cdot}74\,J\,m^{-2}$ and $0{\cdot}77\,J\,m^{-2}$ respectively, were obtained by these workers using the Stillinger–Weber potential. The energy of the {001} interstitial planar defect (model A) is somewhat higher, which makes the {113} habit plane rather than the {001} plane energetically more favourable for the agglomeration of interstitials. HREM images of the {001} extrinsic stacking faults, simulated for different defocus values, are illustrated in fig. 5. These images demonstrate that the effect of the (2×2) reconstruction on the image contrast (a double contrast periodicity with respect to the perfect lattice contrast) can be enhanced or suppressed by choosing the appropriate defocus value. Probably, the {001} interstitial defect in Ge recently reported by Muto and Takeda (1995), who independently revealed model A directly from the analysis of the HREM image (although they reported a fourfold symmetry instead of the correct $\bar{4}$-fold one), has the same structure as the central part of the defect reported earlier by Pasemann *et al.* (1983), where traces of a similar reconstruction are visible.

Fig. 5

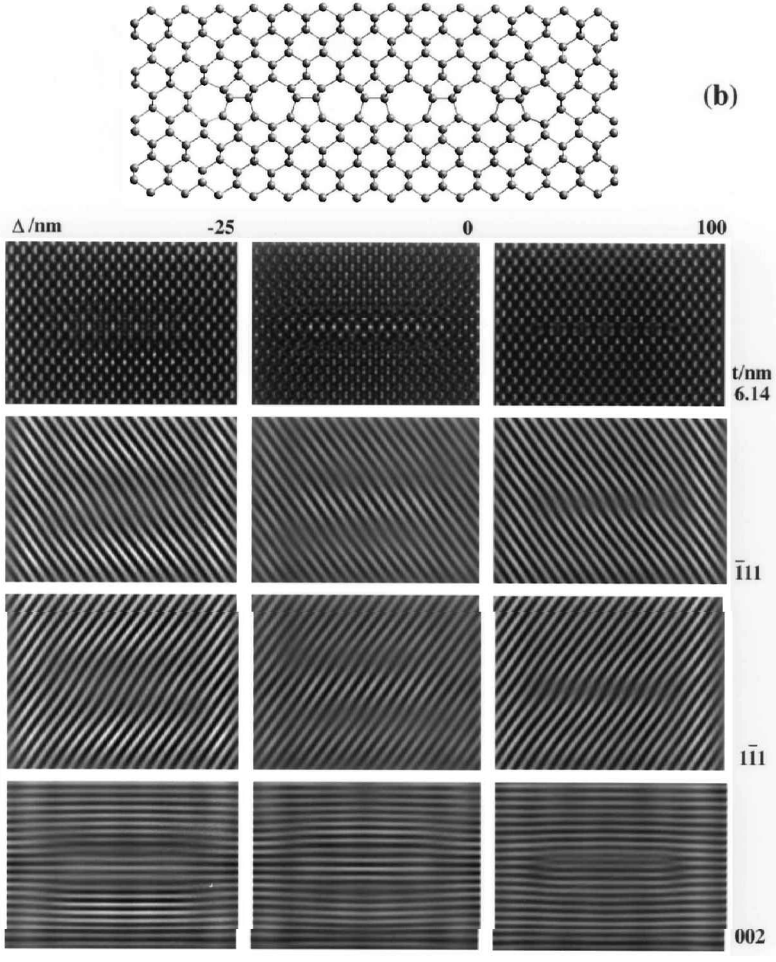

References

Aseev, A. L., Fedina, L. I., Hoehl, D., and Bartsch, H., 1994, *Clusters of Interstitial Atoms in Silicon and Germanium* (Berlin: Akademie).

Bigger, J. R. K., McInnes, D. A., Sutton, A. P., Payne, M. C., Stich, I., King-Smith, R. D., Bird, D. M., and Clarke, L. J., 1992, *Phys. Rev. Lett.*, **69**, 2224.

Burret, A., 1987, *Microscopy of Semiconducting Materials 1987*, Institute of Physics Conference Series No. 87, edited by A. G. Cullis and P. D. Augustus (Bristol: Institute of Physics), p. 39.

Chadi, D. J., 1987, *Phys. Rev. Lett.*, **59**, 1691.

Cheikh, M., Deyehe, M., Hairie, A., Hairie, F., Nouet, G., and Paumier, E., 1991, *Polycrystalline Semiconductors II*, Springer Proceedings in Physics, Vol. 54, edited by J. H. Werner and H. P. Strunk (Berlin: Springer), p. 200.

Conrad, D., Scheerschmidt, K., and Gösele, U., 1996, *Appl. Phys.* A, **62**, 7.

Duesbery, M. S., Joos, B., and Michel, D. J., 1991, *Phys. Rev.* B, **43**, 5143.

Gösele, U., Stenzel, H., Martini, T., Steinkirchner, Conrad, D., and Scheerschmidt, K., 1995, *Appl. Phys. Lett.*, **67**, 3614.

Grell, H., Krause, C., and Grell, J., 1988, *Tables of the 80 Plane Space Groups in Three Dimensions*, INFORMATIK–Information Reporte, Vol. 2 (Berlin: Akademie der Wissenschaften der DDR).

Hornstra, J., 1959, *Physica*, **25**, 409; 1960, *ibid.*, **26**, 198.

Kohyama, M., 1996, *Mater. Sci. Forum*, **207–209**, 265.

Kohyama, M., and Takeda, S., 1992, *Phys. Rev.* B, **46**, 12305; 1995, *ibid.*, **51**, 13111.

Kohyama, M., and Yamamoto, R., 1994, *Phys. Rev.* B, **49**, 17102.

Kohyama, M., Kose, S., and Yamamoto, R., 1993, *Mater. Sci. Forum*, **126–128**, 213.

Mostoller, M., Chisholm, M. F., and Kaplan, T., 1994, *Phys. Rev. Lett.*, **72**, 1494.

Muto, S., and Takeda, S., 1995, *Phil. Mag. Lett.*, **72**, 99.

Parisini, A., and Burret, A., 1993, *Phil. Mag.* A, **67**, 605.

Pasemann, M., Hoehl, D., Aseev, A. L., and Pchelyakov, A. P., 1983, *Phys. Stat. sol. (a)*, **80**, 135.

Phillpot, S. R., and Wolf, D., 1989, *Phil. Mag.* A, **60**, 545.

Ralantoson, N., Hairie, F., Hairie, A., Nouet, G., and Paumier, E., 1993, *Mater. Sci. Forum*, **126–128**, 241.

Stillinger, F. H., and Weber, T. A., 1985, *Phys. Rev.* B, **31**, 5262.

Sutton, A. P., 1991, *Polycrystalline Semiconductors II*, Springer Proceedings in Physics, Vol. 54, edited by J. H. Werner and H. P. Strunk (Berlin: Springer), p. 116.

Sutton, A. P., and Balluffi, R. W., 1995, *Interfaces in Crystalline Materials* (Oxford: Clarendon).

Takeda, S., 1991, *Jap. J. appl. Phys.*, **30**, L639.

Takeda, S., Kohyama, M., and Ibe, K., 1994, *Phil. Mag.* A, **70**, 287.

Tan, T. Y., 1981, *Phil. Mag.* A, **44**, 101.

Tarnow, E., Dallot, P., Bristowe, P. D., Joannopoulos, J. D., Francis, G. P., and Payne, M. C., 1990, *Phys. Rev.* B, **42**, 3644.

Tersoff, J., 1989, *Phys. Rev.* B, **39**, 5586.